CrystEngComm

Accepted Manuscript

ROYAL SOCIETY OF CHEMISTRY

www.rsc.org/crystengcomm

CrystEngComm

COMMUNICATION

Insight into a direct solid-solid transformation: a potential approach to removal of residual solvents†

Received 00th January 20xx,
Accepted 00th January 20xx

DOI: 10.1039/x0xx00000x

www.rsc.org/

Pengpeng Yang[a], Chenguang Lin[a], Wei Zhuang*[a], Qingshi Wen[a], Fengxia Zou[a], Jingwei Zhou[a], Jinglan Wu*[a] and Hanjie Ying*[ab]

Here we report two new crystal forms of adenosine 3',5'-cyclic monophosphate sodium and discovered the direct solid-solid transformation process from its methanol trihydrate (solvate) to its pentahydrate form (hydrate) only mediated by humidity. This findings provide a potential approach to removal of residual solvent in the manufcturing of pharmaceutical and food additives.

Solution crystallization is commonly employed in the separation and purification stages of the industrial production of active pharmaceutical ingredients (APIs) and food additives,[1] and the issues of organic solvent residue is encountered usually and inevitably.[2] How to remove it had always been paid to close attentions because residual solvents influence the quality of products, stability properties and are a potential toxic risk for human health as well.[2-6] For crystalline products, residual solvents exist either on the surface of products, or embed into the crystal lattice. The conventional ways to removal of residual solvents are the freeze drying, heat blowing, vacuum drying, microwave-assisted drying, etc.,[7-9] which may lead to some issues, especially for those compounds developed as hydrates. Mild desorption condition are available for surface residual solvents but less effective for removing completely the solvent molecules incorporated into crystal lattice, while severe conditions tend to break the original packing arrangements and give possibly rise to the variation in solid forms. Thus, development of new effective methods for reliable desorption of residual solvent under the premise of eligible quality of products is of great importance for pharmaceutical and food additives development.

As we all know, hydrates, as one of solid forms, have different properties from those of the corresponding anhydrous species,[10-12] and crystal water molecule acts as "bridge" or "glue" to allow the bulk structure to be more stable.[13-17] Once solvent molecules was incorporated into the crystal lattice as impurities, they can occupy the position of original water. If, thus, one attempts to remove such solvent, on the one hand, desorption or extrusion of them out of crystal lattice is required at first, and on the other hand, it is necessary that new water molecule fill the position so as to ensure to the inherent packing mode.

Nucleotide and its derivatives belongs to the class of polyhydroxyl phosphoryl compounds, and their salts exist mostly in hydrated forms.[16, 18-25] The cases of solvent residue are very common among their manufacturing by solution crystallization. In this report, methanol trihydrate of 3',5'-cyclic adenosine monophosphate sodium (cAMPNa, treatment for diseases of the nervous and respiratory systems Fig. 1), [26, 27] was taken as a representative case. A direct solid to solid transformation mediated by humidity from solvate to hydrate was investigated, in which the desorption of solvent in crystal lattice was achieved, and the original packing arrangements of solid form was retained simultaneously.

Single crystal of solvate cAMPNa·CH_3OH·$3H_2O$ was grown from methanol aqueous solution at an initial supersaturation (S=2.79, relevant solubility data was seen in our previous report[27]).

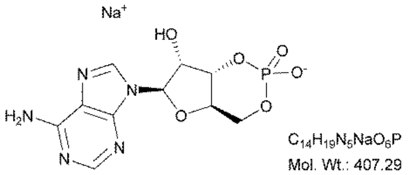

Fig. 1. The molecular formula of 3',5'-cyclic monophosphate sodium (cAMPNa).

The typical morphology was seen in Fig. 2. Another new single crystal of pentahydrate cAMPNa·$5H_2O$ can be obtained by controlling crystallization temperature in acetone aqueous solution (corresponding S=1.54~1.71 at the initial stage). The morphology of resulted crystals was similar to that of

---

[a] National Engineering Technique Research Center for Biotechnology, College of Biotechnology and Pharmaceutical Engineering, Nanjing Tech University, No. 30, Puzhu South Road, Nanjing 211816, PR China. Tel.: +86 25 86990001; fax: +86 25 58133398. E-mail address: yinghanjie@njtech.edu.cn (H. Ying).
[b] State Key Laboratory of Materials-Oriented Chemical Engineering. Xin Mofan Road 5, Nanjing 210009, PR China

† Electronic Supplementary Information (ESI) available: Experimental section, hydrogen bond parameters and sodium coordination scheme in pentahydrate and methanol trihydrate, asymmetric cell diagram and the compositions of main samples. CIFs and structure factor files, CheckCIF report. CCDC 1026499, 1026507. See DOI: 10.1039/x0xx00000x

methanol trihydrate. Detailed crystallographic protocol was seen in ESI.

After the preparation of crystals, suitable crystals were selected for the structure determination of single crystal X-ray diffraction. And the rest of products were collected by filtration, air-dried at room temperature, grind and used for subsequent experiment after identification. Approximately 0.2 x 0.2 x 0.2 mm^3 of crystal was mounted on a glass fiber and transferred to a Bruker APEX-II CCD diffractometer equipped with Mo K_α radiation (graphite monochromator, λ = 0.71073 Å) and Oxford Cryostream (Oxford Cryosystems) open-flow nitrogen cryostat for sample temperature control. The data were collected to a maximum of 2θ = 50° at 296 K, and were corrected by applying multi-scan method. Structures were solved by direct method and refined by full-matrix least-squares method on F^2 using SHELX-97.[28] All non-hydrogen atoms were refined anisotropically. Hydrogen atoms were placed in calculated positions and refined with isotropic thermal parameters. Final R values: R = 0.0480, wR_2= 0.1279 for cAMPNa·CH_3OH·$3H_2O$ and 0.0499, 0.1397 for cAMPNa·$5H_2O$. More detailed crystallographic data are available in Tables 1, S1 in ESI and from the Cambridge Crystallographic Data Center (CCDC 1026507 and 1026499). Diamond[29], Materials studio[30] and Mercury software[31] was used for crystal structure analysis and simulation of powder X-ray diffraction patterns based on crystal structure data.

From the table 1, it was found that the structures of two crystal forms of cAMPNa were isostructural materials. Their thermal ellipsoids of asymmetric cell with a 30% probability were shown in ESI Figs. S1 and S2, and the molecular packing diagram of methanol trihydrate viewed along *a* axis was shown in Fig. 3 (the molecular packing of pentahydrate was seen in Fig. S3). For two pseudo-polymorph, the glycosidic bonds are anti, and the conformations of the furanose rings are C9-exo C8-endo. The purine bases are planar and the six-membered phosphate rings present in a chair conformation, as the case of monoclinic tetrahydrate of cAMPNa.[18] The base fragments stack in an antiparallel fashion with a spacing of approximately 3.3 Å to form a molecular column, giving alternating orientations along the stack. The crystal packing is strongly influenced by the cations. Sodium ions are coordinated by six Na-O bonds, interacting with four water and two different cAMP molecules. The resulting Na-O-Na polymer forms a columnar structure down the *b* axis surrounded by the phosphate groups. The methanol molecule was placed between the moieties of ribose of two neighboring molecular layers (see Figs. 3, S3, and S4).

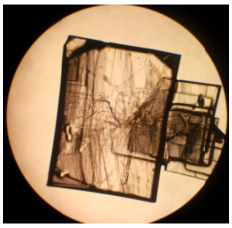

Fig. 2. The morphology of orthorhombic methanol trihydrate. (optical microscope, 10 × 4)

Table 1. Structural information of two new crystal forms of cAMPNa.

Solid form	cAMPNa·$5H_2O$	cAMPNa·CH_3OH·$3H_2O$
Crystal system	Orthorhombic	Orthorhombic
Space group	$P2_12_12_1$ (No. 19)	$P2_12_12_1$ (No. 19)
a(Å)	6.5585 (12)	6.5021(10)
b(Å)	7.0470 (13)	7.0943 (11)
c(Å)	38.869(7)	39.198(6)
V [$Å^3$]	1796.4(6)	1808.1(5)
Z/Z′	4/1	4/1
R	0.0499	0.0480
wR_2	0.1397	0.1279
Goodness-of-fit (on F^2)	1.10	1.16
Na^+ coordination number	6	6
Hydrogen bond water number	3	1
Coordinated water number	2	2
Water & solvent occupied volume fraction in cell	9.07%	9.13%
Theoretical water content	20.42%	12.36%

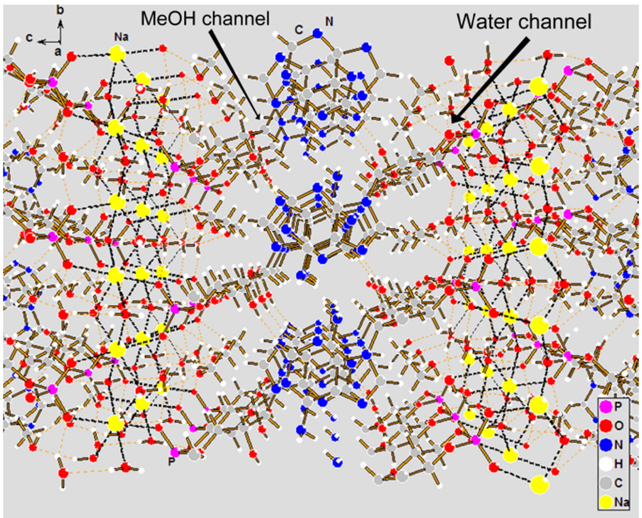

Fig. 3. The packing perspective diagram of methanol trihydate of cAMPNa along a-axis.

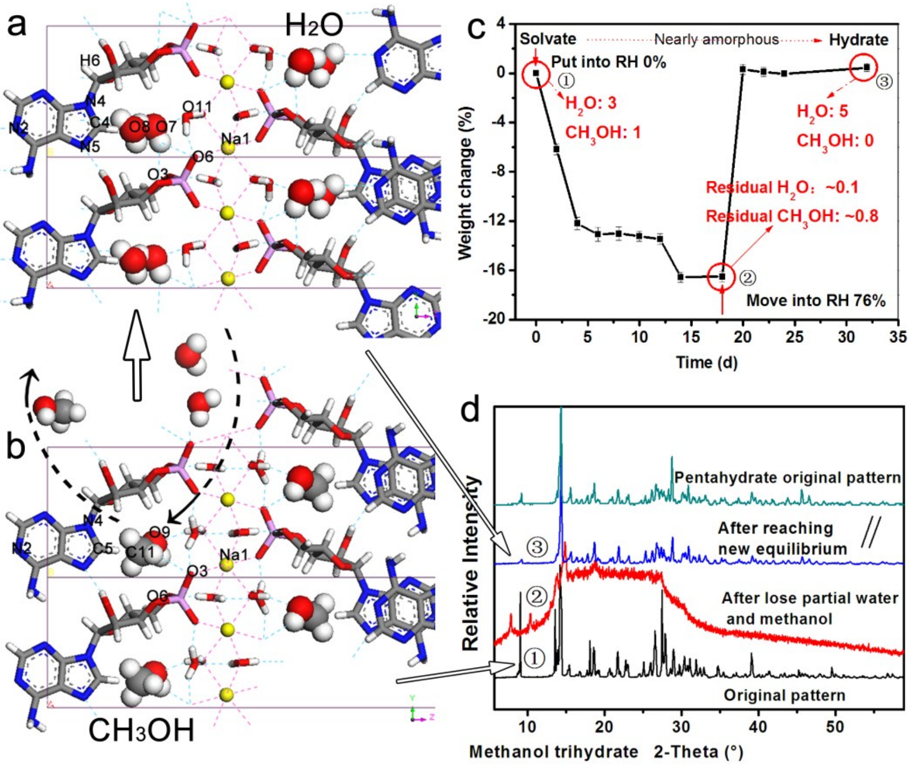

Fig. 4. The solid-solid transformation from solvate cAMPNa·CH_3OH·$3H_2O$ to hydrate cAMPNa·$5H_2O$ mediated by humidity. (a) and (b) were the packing structures of solvate and hydrate, showing the location of two crystal water molecules and replaced methanol molecule in two lattice; (c) was the process of removal of crystal water/methanol and uptake of external water molecules, accompanying the crystal form conversion (① original methanol trihydrate crystalline powder, ② after treatment in RH 0% conditions, ③ after treatment in RH 76% conditions). The red text indicates the number of solvent per cAMP molecule in crystal lattice; (d) was the PXRD patterns for three sampling points.

The humidity sensitivity experiment under different RH conditions at room temperature was carried out to examine the stability of the two crystal forms. Approximately 180 mg (fine ground samples) of each of crystals was placed in Petri dish with 5 cm diameter and stored in humidity chamber for 13 weeks. To provide a variety of relative humidity values for humidity stability experiment, saturated salt solutions and P_2O_5 were used. The salts used for this experiment and the corresponding RH values were $MgCl_2$ (32%), NaCl (76%), K_2SO_4 (98%), and P_2O_5 solid powder (~0%).[32] After the test period, the stored samples were analyzed in gravimetry and composition. Each of crystal forms was repeated three times. The results indicated methanol trihydrate and pentahydrate of cAMPNa were stable at 32-76% relative humidity (RH), remaining identical composition, seen in ESI Tables S3, S4. However, they tended to lose water or methanol at lower RH conditions (<10%), were hygroscopic at high RH and finally completely deliquesced to a transparent liquid drop at RH 98%. Furthermore, the powder of methanol trihydrate was subjected to low RH (e.g., 0%) initially for about half a month, until the sample weight ceased to decrease. Then, the sample was transferred and subjected to RH 32-76% until equilibrium was attained. The whole process was performed at room temperature and variations in weight was recorded at regular intervals. At three sampling points (see Fig. 4 ①-③), the solid structure were evaluated using powder X-ray diffraction (PXRD). The absolute contents of residual water and methanol of the sample were determined by Karl Fischer method (Metrohm 870 KF Titrino plus, Switzerland) and gas chromatograph (7890A, Agilent, Wilmington, ED, USA) equipped with a flame ionization detector (FID) respectively, and converted to be corresponding solvent number per cAMP in crystal lattice. The ESI detailed the experimental and computational details (Table S4), and the results were shown in Fig. 4.

We noted that the PXRD pattern of the sample after the experiment was remarkably different from that of the original solvate, whereas in agreement with that of pentahydrate (see Fig. 4d). Accordingly, we speculated that it was possible that the initial solvate cAMPNa·CH_3OH·$3H_2O$ had been transformed to the hydrate cAMPNa·$5H_2O$ after undergoing the humidity process. And methanol in original crystal lattice was likely to be removed and replaced by water molecules, which was further confirmed by the analysis of sample composition (see Fig. 4c, Table S4). This phenomenon is common among metal-organic frameworks (MOFs) and resembles the desorption/adsorption of resins, dendrimers, or clathrate complexation to some extent[33, 34], in regard to the removal of methanol and uptake of water by solvate and desolvate, but reported less frequently for non-polymeric structures.[35, 36] For the cAMPNa solvate, although the Na-O-Na coordination polymer and the base packing provide a definite framework to the structure, it appears to be some different from the typical physical desorption/sorption of general resins because the release/uptake of crystal water and methanol was accompanied by larger bulk reorganization. The solid structure was in a partially amorphous with the loss of solvent, yet the crystallinity would turn to increase with uptake of water molecules (see the patterns of sampling point ② in Fig. S4d). As such, gas sorption theories such as Langmuir isotherm model assuming monolayer adsorption on a homogeneous surface, Freundlich isotherm model assuming adsorption on a heterogeneous surface, and Brunauer-Emmett Teller isotherm model for multilayer adsorption could not be available.[37, 38] Furthermore, removal of the guest molecules did not leave detectable pores (as would be expected for clathrates), and the sample exhibited a nonporous behaviour in N_2 adsorption-desorption experiments (see ESI). This indicates that the “pore size” was smaller than N_2 with a dynamic diameter of 3.6 Å, but may be larger than that of gaseous water molecules (2.7~3.2 Å). Certainly, the observed effects may be related to the affinity of gas molecules to the surface, apart from the steric effects.

Crystal water or methanol molecule are capable of forming hydrogen and coordination bonds in the lattice, as noted by analysis of single crystal data (Fig. S4a and Tables S6, S7). The occupied volume of three water molecules and one methanol molecule is 490.88 Å³ in the $cAMPNa{\cdot}CH_3OH{\cdot}3H_2O$ crystal lattice, and close to that of five water molecules 472.91 Å³ in the $cAMPNa{\cdot}5H_2O$ lattice (Connolly radius was set to 1.0 Å, van der Waals scale factor was 1.0 Å, and grid interval was 0.75 Å).[39] The location and surroundings of five water molecules were extremely similar to that of both three water molecules and one methanol molecule, thus they likely exhibited analogous bonding modes (see Fig. 4a-b). Moreover, both the space group and packing mode were identical for the two solid forms. The actual volume of one methanol molecule (67.2 Å³) is quite similar to that of two water molecules (32.6 x 2 = 65.2 Å³), and the conformation of the host cAMP molecule and its packing arrangements were only slightly altered from the solvate to the hydrate (the torsion angles, χ_{CN}, were 63.29° and 59.75°, the distance between adjacent two base plane, 3.256 Å and 3.293 Å, Fig. 5). The energy gap of single $cAMP^-$ in two crystal lattices before and after the transformation was only 1.79 kJ/mol (DNP basis set, PBE functional, $Dmol^3$, Material studio 6.0)[30, 40]. In other words, the transformation from the solvate $cAMPNa{\cdot}CH_3OH{\cdot}3H_2O$ to the hydrate $cAMPNa{\cdot}5H_2O$ can be regarded as a replacement reaction mediated by humidity, as described in equation 1.

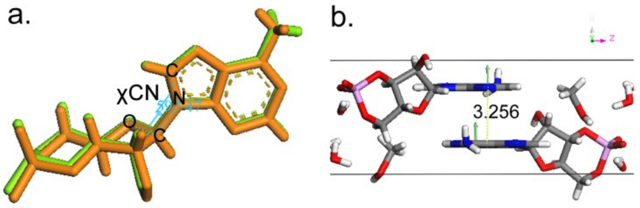

Fig. 5. (a) The minor difference in the conformation of host molecule $cAMP^-$ of methanol trihydrate of cAMPNa and its pentahydrate; (b) the distance between adjacent two base plane,3.256 Å for methanol trihydrate and 3.293 Å for pentahydrate.

$$cAMPNa{\cdot}CH_3OH{\cdot}3H_2O\ (s) + 2H_2O\ (g) \longrightarrow cAMPNa{\cdot}2H_2O{\cdot}3H_2O\ (s) + CH_3OH\ (g) \qquad \textbf{Eq. 1}$$

The hydroxyl group of methanol binds with one molecule of crystal water and O(P-O) *via* two strong hydrogen bonds, as depicted in Figs. 3b, S4a. The loss of crystal water and methanol in the crystal lattice of methanol trihydrate occurred step-wise under RH 0% conditions, and the desorption rate of methanol was less than that of crystal water (at sampling point ②, the absolute content of methanol and water of sample were 6.77% and 0.48%, equivalently approximately 0.8 methanol and 0.1 water per cAMP respectively, and equivalently loss of 20% of methanol and 97% of water as well, Fig. 4c and Table S4). After methanol and water were partially removed and the sample was transferred to RH 32-76%, gaseous water molecules in surroundings could absorb onto the crystal surface, get into the crystal lattice, and restructure the host species. Moreover, due to the affinity and concentration of water molecule, two new water molecules can replace the original methanol molecule, and bond with O3 (furanose ring), O6 (P-O), and N2 (6-membered pyrimidine ring) via hydrogen bonds. As such, methanol can be replaced by water completely until thermodynamic equilibrium is attained. Besides, the methanol and non-coordinated water molecules are located in channels, which facilitates solvent exchange. It should be mentioned that the uptake rate of water at RH 32% was significantly less than that of RH 76%. Some requirements should be met for the conversion of this kind to occur in solid formulations: (i) nearly equal size of molecules to be replaced; (ii) potential for bond formation in crystal lattice.

The conversion condition of solvate to hydrate referred to in this study was static humidity environment, and the duration time of several days were required . In fact, if low humidity condition was given by dynamics dry air flow, and

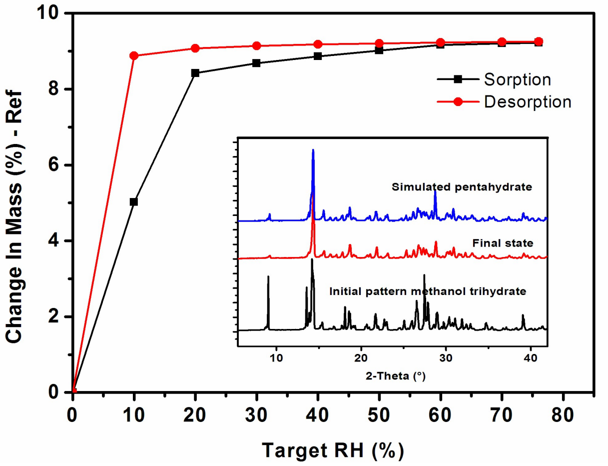

Fig. 6. Dynamic vapor sorption isotherm plot of methanol trihydrate. Change in sample mass was calculated by using the minimum at RH 0% as the reference point.

dynamics water vapor with proper relative humidity was used in the aforementioned second stage, the conversion of solvate to hydrate (that is the replacement of methanol in the lattice) will be significantly accelerated, which was corroborated by the dynamic vapor sorption (DVS) experiment. (It was conducted using a DVS Intrinsic dynamic gravimetric water sorption analyser (SMS Ltd., London, UK) at 25.0±0.1 ℃. About 20 mg of samples were placed in the quartz sample pan. The RH was decreased from 76% to 0% in the desorption process and then increased from 0% to 76% in the sorption and exchange process with the step size of 10% RH. The sample was equilibrated at each step with the equilibration criterion of either dm/dt ≤ 0.002 %/min at the level of no less than 10 min of duration time or a maximum equilibration time of 3 h.[17] The solids before and after DVS tests were subjected to powder XRD measurements to monitor possible solid-form transformation, see Fig. 6). In this case, the whole transformation process can be completed within several hours.

In conclusion, the humidity-mediated method in this report allows the methanol in cAMPNa lattice to be removed completely, and enable the its methanol trihydrate to be converted to its pentahydrate. This may provides a potential possibility for how to deal with the residual solvent simply and effectively for some crystal products, as well as help to the knowledge of solid-solid conversion behaviors. Further investigation on other solvates transformation and wiping off residual organic solvent of hydrates product by this approach are currently underway.

Acknowledgements

This work was supported by the National Basic Research Program of China (973) (2013CB733602), Major Research Plan of the National Natural Science Foundation of China (21390204, 21506090), Program for Changjiang Scholars and Innovative Research Team in University (IRT_14R28), and Priority Academic Program Development of Jiangsu Higher Education Institutions (PAPD).

References

1 S. K. Poornachary, P. S. Chow and R. B. H. Tan, *Cryst. Growth Des.*, 2008, **8**, 179-185.
2 M. Mirmoghaddam, M. Kaykhaii and H. Yahyavi, *Anal. Methods*, 2015, **7**, 8511-8523.
3 C. B'Hymer, *J. Chromatogr. Sci.*, 2008, **46**, 369-374.
4 M. A. Farajzadeh, L. Goushjuii, D. Djozan and J. K. Mohammadi, *J. Sep. Sci.*, 2012, **35**, 1027-1035.
5 G. Nichols and C. S. Frampton, *J. Pharm. Sci.*, 1998, **87**, 684-693.
6 E. V. Boldyreva, V. A. Drebushchak, I. E. Paukov, Y. A. Kovalevskaya and T. N. Drebushchak, *J. Therm. Anal. Calorim.*, 2004, **77**, 607-623.
7 B. S. Kim and J. H. Kim, *Korean J. Chem. Eng.*, 2008, **25**, 108-111.
8 C. G. Lee and J. H. Kim, *Process Biochem.*, 2015, **50**, 1031-1036.
9 J.-Y. Lee and J.-H. Kim, *Process Biochem.*, 2013, **48**, 545-550.
10 D. Braga, F. Grepioni and L. Maini, *Chem. Commun.*, 2010, **46**, 6232-6242.
11 V. André, L. Cunha-Silva, M. T. Duarte and P. P. Santos, *Cryst. Growth Des.*, 2011, **11**, 3703-3706.
12 J.-B. Arlin, R. M. Bhardwaj, A. Johnston, G. J. Miller, J. Bardin, F. MacDougall, P. Fernandes, K. Shankland, W. I. David and A. J. Florence, *CrystEngComm*, 2014.
13 A. Bērziņš, E. Skarbulis, T. Rēķis and A. Actiņš, *Cryst. Growth Des.*, 2014, **14**, 2654-2664.
14 S. Aitipamula, P. S. Chow and R. B. H. Tan, *Cryst. Growth Des.*, 2014, **14**, 6557-6569.
15 S. Aitipamula, V. R. Vangala, P. S. Chow and R. B. H. Tan, *Cryst. Growth Des.*, 2012, **12**, 5858-5863.
16 M. Dracinsky, M. Sala and P. Hodgkinson, *CrystEngComm*, 2014, **16**, 6756-6764.
17 L. Wang, X. Wen, P. Li, J. Wang, P. Yang, H. Zhang and Z. Deng, *CrystEngComm*, 2014, **16**, 8537-8545.
18 K. I. Varughese, C. T. Lu and G. Kartha, *J. Am. Chem. Soc.*, 1982, **104**, 3398-3401.
19 T. P. V. Seshadri, M. A., *Curr. Sci.*, 1974, **43**, 110-111.
20 T. P. Seshadri, M. A. Viswamitra and G. Kartha, *Acta Crystallogr., Sect. B: Struct. Sci.*, 1980, **36**, 925-927.
21 E. Shefter and K. N. Trueblood, *Acta Crystallogr.*, 1965, **18**, 1067-1077.
22 Y. Sugawara, A. Nakamura, Y. Iimura, K. Kobayashi and H. Urabe, *J. Phys. Chem. B*, 2002, **106**, 10363-10368.
23 Y. Sugawara, H. Urabe, K. Kobayashi, Y. Iimura and H. Iwasaki, *Mol. Cryst. Liq. Cryst. Sci. Technol., Sect. A*, 1996, **276**, A255-A258.
24 E. A. Brown and C. E. Bugg, *Acta Crystallogr., Sect. B: Struct. Sci.*, 1980, **36**, 2597-2604.
25 E. A. Brown and C. E. Bugg, *J. Cryst. Mol. Struct.*, 1980, **10**, 19-30.
26 A. Rinat, T. Einat, J. H. Jasmine, Z. Evelyne, A. Ninette, P. Orit, R. Gideon, G. Eithan and H. Alik, *Cancer Res.*, 2004, **64**, 1338-1346.
27 P. Yang, Q. Wen, J. Wu, W. Zhuang, Y. Zhang and H. Ying, *Ind. Eng. Chem. Res.*, 2014, **53**, 10803-10809.
28 G. M. Sheldrick, *Acta Crystallogr., Sect. A: Found. Crystallogr.*, 2008, **64**, 112-122.
29 K. Brandenburg, Diamond Version 3.2e (Crystal Impact GbR, Bonn, Germany).
30 Materials Studio software 6.0 (Accelrys Inc., 2012)
31 C. F. Macrae, I. J. Bruno, J. A. Chisholm, P. R. Edgington, P. Mccabe, E. Pidcock, L. Rodriguez-Monge, R. Taylor, J. V. D. Streek and P. A. Wood, *J.appl.cryst*, 2008, **41**, 466-470.
32 L. Greenspan, *J. Res. Natl. Bur. Stand. (U. S.)*, 1977, **81**, 81--89.
33 G. J. Kemperman, R. de Gelder, F. J. Dommerholt, P. C. Raemakers-Franken, A. J. H. Klunder and B. Zwanenburg, *Chem. Eur. J.*, 1999, **5**, 2163-2168.
34 A. W. Bosman, H. M. Janssen and E. W. Meijer, *Chem. Rev.*, 1999, **99**, 1665-1688.
35 G. P. Bettinetti, M. R. Caira, M. Sorrenti, L. Catenacci, M. Ghirardi and L. Fabian, *J. Therm. Anal. Calorim.*, 2004, **77**, 695-708.
36 M. Shiraki, *J. Pharm. Sci.*, 2010, **99**, 3986-4004.
37 P. Kumar, W. L. Pei, S. Kale, S. Johnson, V. Pareek, R. Utikar and A. Lali, *J. Chromatogr. A*, 2014, **1356**, 105–116.
38 A. B. Thompson, S. J. Cope, S T Dallas and J. M. Notestein, *Langmuir*, 2011, **27**, 11990-11998.
39 M. L. Connolly, *Science*, 1983, **221**, 709-713.
40 J. P. Perdew, K. Burke and M. Ernzerhof, *Phys. Rev. Lett.*, 1996, **77**, 3865-3868.